Cancer Chemother Pharmacol (2013) 71:473–480
DOI 10.1007/s00280-012-2032-6

ORIGINAL ARTICLE

Response to trastuzumab by HER2 expressing breast tumour xenografts is accompanied by decreased Hexokinase II, glut1 and [^{18}F]-FDG incorporation and changes in ^{31}P-NMR-detectable phosphomonoesters

Tim A. D. Smith · M. Virginia C. L. Appleyard · Sheila Sharp · Ian N. Fleming · Karen Murray · Alastair M. Thompson

Received: 28 August 2012 / Accepted: 13 November 2012 / Published online: 24 November 2012

Abstract
Purpose Trastuzumab, effective in about 15 % of women with breast cancer, downregulates signalling through the Akt/PI3K and MAPK pathways. These pathways modulate glucose and phospholipid metabolism which can be monitored by [^{18}F]FDG-PET and ^{31}P-NMR spectroscopy, respectively. Here, the relationship between response of HER-2 overexpressing tumours and changes in [^{18}F]-FDG incorporation and ^{31}P-NMR-detectable phosphomonoesters were examined.
Experimental Xenografts derived from HER2-overexpressing MDA-MB-453 human breast tumour cells were grown in SCID mice, treated with trastuzumab for 15 days, then [^{18}F]-FDG uptake determined and ^{31}P-NMR carried out on chemical extracts of the tumours. Western blots were carried out to determine protein expression of Hexokinase II and glut1.
Results [^{18}F]-FDG incorporation, Hexokinase II and glut1 protein expression and the concentration of phosphocholine and phosphoethanolamine in chemical extracts subjected to ^{31}P-NMR were significantly decreased in the xenografts in the trastuzumab-treated mice compared with xenografts from the PBS-injected group.
Conclusions Changes in FDG incorporation and ^{31}P-NMR spectral changes can accompany response of HER2-expressing breast cancer xenografts to trastuzumab. This is the first study to show parallel changes in [^{18}F]FDG- and ^{31}P-NMR-detectable metabolites accompany response to targeted anticancer treatment.

Keywords [^{18}F]FDG · ^{31}P-NMR · Trastuzumab · Hexokinase · Xenograft

T. A. D. Smith (✉) · I. N. Fleming
Division of Applied Medicine, School of Medicine and Dentistry, University of Aberdeen, Biomedical Physics Building, Foresterhill, Aberdeen AB25 2ZD, UK
e-mail: t.smith@abdn.ac.uk

M. V. C. L. Appleyard · S. Sharp · K. Murray · A. M. Thompson
Dundee Cancer Centre, Ninewells Hospital & Medical School, University of Dundee, Dundee DD1 9SY, UK

Introduction

Studies have consistently shown that decreased [^{18}F]-FDG incorporation during the course of treatment demonstrates tumour response to cytotoxic chemotherapy [1–4]. Changes in tumour [^{18}F]-FDG incorporation in response to cytotoxics is generally considered to reflect changes in viable cell number and decreased proliferation rates of responding tumours. Novel targeted anticancer drugs which include antiHER2 compounds such as trastuzumab bind to receptors which are uniquely overexpressed in different cancer types. Receptor binding results in receptor internalisation and therefore causes diminished cell surface expression and down-regulation of intracellular signalling pathways [5]. Pathways downstream of HER2 include Akt and MAPK which influence glycolysis [6] through HIF1 [7]. Thus, the level of activation of HER2 is closely associated with glucose utilisation so its deactivation would be expected to reduce [^{18}F]-FDG incorporation.

Several studies suggest that decreased [^{18}F]-FDG incorporation predicts response of breast tumours [8] and xenografts [9] derived from breast cancer cells, to anti-HER2 treatments including the antiHER 2 antibody trastuzumab. However, the results from a study based on a xenograft and a transgenic murine cancer model [10] concluded that glucose metabolism was not sufficiently

decreased by treatment with trastuzumab to induce detectable changes in [^{18}F]-FDG incorporation but they did not assess changes in the expression of glucose handling proteins. To further investigate the relationship between response to trastuzumab and glucose utilisation, we have measured [^{18}F]-FDG incorporation, and the expression of two proteins which have a primary role in glucose metabolism, Hexokinase II (HK II) and glut1, by xenografts derived from the HER2-overexpressing cell line MDA-MB-453 during response to treatment with trastuzumab.

Changes in phospholipid metabolism, detectable using ^{31}P-NMR spectroscopy commonly accompany tumour response to therapy [11, 12]. Hybrid PET/MR imaging systems now commercially available [13] have the potential to measure tumour [^{18}F]-FDG incorporation and acquire ^{31}P-NMR spectral data in the same clinical session potentially providing a more definitive assessment of response to trastuzumab. Mindful of these developments and the inconsistency in [^{18}F]FDG-PET to detect response of xenografts to trastuzumab, we have subjected chemical extracts prepared from the trastuzumab-treated and control MDA-MB-453 xenografts to high-resolution ^{31}P-NMR spectroscopic examination.

Materials and methods

Materials

All chemicals were purchased from Sigma-Aldrich Chemical Company (Poole UK) unless otherwise stated. The MDA-MB-453 cell line was purchased from American Type Cell Culture collection (ATCC) through LGC Standards (Teddington UK). [^{18}F]FDG was acquired from the PET Unit at the Clinical Research Centre at Dundee's Ninewells Hospital.

Methods

Xenograft growth and treatment with trastuzumab

All animal work was approved by and carried out within the UK Home Office guidelines on a Home Office Project licence by staff holding current Personnel Home Office licences. Fourteen females, 2-month-old SCID mice, with and average weight of 24 g (±2.1 g) were inoculated subcutaneously into the right flank with 2×10^6 MDA-MB-453 HER2-overexpressing human breast tumour cells in 0.1 ml of saline.

The xenografts were measured by callipers every 3 days and the volume determined using the formula: $V = 4/3\pi[(w + l)/4]^3$ [V = volume (mm^3), w = width (mm), l = length (mm)]. Tumours were allowed to develop until at least 50 mm^3 in volume. A group of 7 mice were treated i.p. with trastuzumab according to the schedule: 4 mg/kg on day 1 followed by maintenance doses of 2 mg/kg on days 8 and 15. These doses are similar to those used clinically (on an mg/kg body weight basis) [14]. The remaining group of 7 mice were injected with 0.2 ml of phosphate-buffered saline (PBS) on days 1, 8 and 15. The mice were fed ad libitum during the treatment period.

Determination of [^{18}F]-FDG incorporation

Before the administration of [^{18}F]-FDG, the mice were fasted overnight (water ad libitum), then allowed to acclimatise to the radioactivity suite on a warm pad at 37 °C for 1 h. They were then administered i.p. with [^{18}F]FDG (1 MBq in 0.1 ml of saline). One hour later, they were killed and blood was taken and weighed. It has been shown [15] that the distribution of ^{18}F-FDG after 45–60 min in mice injected i.p. is similar to that in mice injected i.v. This was also the administrative route chosen by McLarty et al. [9] who imaged after 1 h. Tumour tissue was rapidly excised and plunged into liquid nitrogen within 1 min of killing. The samples were briefly (<5 min) removed from liquid nitrogen to allow radioactive uptake to be determined on a gamma counter set for 511 keV.

Extraction of metabolites from tumour tissue

Frozen tumour tissue was ground to a fine powder in a pestle and mortar under liquid N_2. The powder was then added to a pre-weighed 1 ml volume Douce homogeniser (Fisher scientific, UK), then reweighed to determine the tumour tissue weight. After addition of 10 µl of a 0.4-M solution of EDTA and an ice-cold mixture of methanol and chloroform (2:1) (0.375 ml per 100 mg of tissue), the tissue was homogenised and the mixture left for 60 min on ice. Chloroform (0.125 ml per 100 mg tissue) followed by 10 mM Tris buffer at pH 7.0 (0.125 ml per 100 mg tissue) was then added to the mixture which was then centrifuged at 1,000*g* for 15 min at 4 °C. The aqueous (upper) phase was then removed and after addition of 0.15 µmol of 1-aminopropylphosphonic acid, the sample was stored at −20 °C until the ^{31}P-NMR measurement was carried out.

^{31}P-NMR spectroscopy

To the samples was added 60 µl of D_2O and the total volume made up to 0.6 ml by addition of water. NMR analysis was carried out on a Varian 600 MHz spectrometer operating at 242.83 MHz for ^{31}P with a ^{1}H decouple of 599.87 MHz. The parameters for each acquisition were: sweep width 104.2 kHz; acquisition time 1.258 s;

relaxation delay 1 s; pulse angle 45°. All acquisitions were made at 25 °C. Metabolite identities were verified by repeating the NMR measurement after addition of commercially available compounds. At least 25,000 scans were acquired for each sample.

To check the recovery of metabolites during the extraction process, a 60-µl sample of a solution of commercially available PMEs and PDEs at similar concentrations to those found in xenograft tissue was subjected to a mock extraction process carried out as for the xenograft tissue. ^{31}P-NMR scans from the standard and the mock extract demonstrated that the recovery of each metabolite was almost quantitative (>96 %). Comparison of the metabolite concentrations in the standard solution with the values derived from the NMR measurements demonstrated that the average measurement accuracy for the metabolites was of 95 %.

Western blot

Tumours (4 control and 4 trastuzumab-treated) were freeze thawed twice in liquid N_2 prior to processing in a mortar and pestle. Tumour fragments were resuspended in ice-cold lysis buffer [50 mM Tris, pH 7.4, 250 mM NaCl, 5 mM EDTA (ethylene diamine tetra-acetic acid), 0.1 % Triton X-100, 0.1 % SDS, 1 mM Na orthovanadate, 2 mM Na pyrophosphate, protease inhibitors and 0.1 mM dithiothreitol], then sonicated (3 × 5 s bursts) with a probe sonicator. Homogenates were centrifuged at 5,000*g* for 10 min to pellet insoluble material. The protein content of each sample was determined using the Bicinchoninic acid (BCA) assay (Sigma-Aldrich).

Lysates (15 µg protein per well) were resolved on 4–12 % gradient acrylamide Bis–Tris gels (Invitrogen, Paisley, UK). Proteins were transferred to Immobilon-P polyvinylidene difluoride (PVDF) membranes (Millipore) at 30 V for 1.5 h (Bio-Rad comb and glass plates, Invitrogen ZOOM Dual Power, UK) Membranes were blocked for 1 h at room temperature in phosphate-buffered saline containing 0.1 % (vol/vol) Tween 20 (PBST) and either 5 % (wt/vol) fat-free dried milk (Hexokinase II or β-actin) or 2 % (wt/vol) BSA (GLUT1). Membranes were probed overnight at 4 °C with the following antibodies: HK II (Santa Cruz Biotechnology) at 1:1,000 dilution in 3 % (wt/vol) milk in PBST; glut1 (Millipore) at 1:1,000 dilution in 2 % (wt/vol) BSA in PBST; β-Actin (Abcam, Cambridge UK) at 1:5,000 dilution in 3 % (wt/vol) milk in PBST. Membranes were washed four times in PBST prior to a 1-h incubation with the appropriate horseradish-peroxidase-conjugated secondary antibody (Santa Cruz Biotechnology) at 1:5,000 dilution in PBST containing 3 % (wt/vol) dried milk. Membranes were washed four times in PBST before antibody detection using an enhanced chemiluminescence kit for horseradish peroxide (EZ-ECL) reagent (Geneflow Ltd). Images were captured using a Fluor-S multiimager (Bio-Rad, UK) using Quantity 1 software. Densitometries of target proteins were determined using ImageJ (National Institutes of Health).

Statistics

The Student's *t* test was used to determine statistically significant differences between means. The results of the *t* test are described as ($t = x$, $p < y$), where *t* is the value for the *t* test and *p* is the probability level that the means differ significantly.

Results

Figure 1 shows the mean volume of each xenograft relative to its volume at the start of treatment during after 4, 6, 8, 11 and 13 days of treatment with trastuzumab or PBS. Xenografts derived from trastuzumab-treated mice declined in size compared with PBS-treated (controls) relative to size at day 1 of treatment (Fig. 1). The change in tumour size at each time point was significantly lower in the treated group compared with the controls for 4 days ($t = 5.03$, $p < 0.001$), 6 days ($t = 5.6$, $p < 0.001$), 8 days ($t = 5.13$, $p < 0.001$), 11 days ($t = 4.12$, $p < 0.005$) and 13 days ($t = 4.42$, $p < 0.005$) of treatment with trastuzumab. By day 13, the tumours in the control group were on average 20 % larger than on day 1 whilst tumours in the trastuzumab-treated group were on average only 40 % the size on day 1.

The mean [^{18}F]FDG uptake (per gram of tumour/injected dose) in the control and trastuzumab-treated mice is shown in Fig. 2. The incorporation of [^{18}F]FDG was

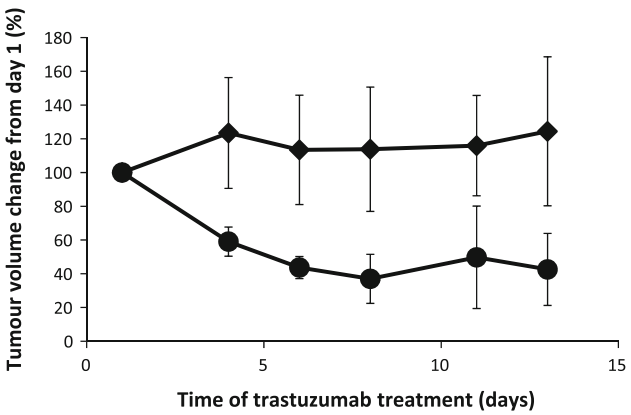

Fig. 1 Change in tumour volume during treatment with trastuzumab (*filled circles*) or PBS (*filled diamonds*) (*Y* axis: The volume of each tumour was calculated at each time point relative to its volume at the start of treatment)

significantly reduced ($t = 2.22$, $p < 0.04$) by tumour tissue in mice treated with trastuzumab for 15 days compared with control mice. [^{18}F]FDG incorporation was also significantly reduced in the trastuzumab-treated mice when expressed as [^{18}F]FDG uptake by tumour relative to blood ($t = 2.4$, $p < 0.04$). [^{18}F]FDG incorporation per gram tissue by tumours in the trastuzumab-treated animals was on average 53 % of that by tumours in the untreated group.

Western blot (Fig. 3) revealed that HK II and glut1 protein expression was significantly ($t = 2.85$, $p < 0.05$ and $t = 3.84$, $p < 0.01$, respectively) lower in the trastuzumab-treated xenografts (HK II: 9.4 ± 6.6 and glut1: 75 ± 20, respectively) compared with controls (HK II: 19 ± 1.4 and glut1: 115 ± 5.8, respectively).

Figure 4a, b shows a typical ^{31}P-NMR spectrum of aqueous extracts prepared from MDA-MB-453 xenografts from control and trastuzumab-treated mice, respectively. The standard of 1-aminopropylphosphonic acid resonates at 11.8 ppm. The two larger peaks in the phosphomonoester (PME) region were identified as phosphoethanolamine (PE) and phosphocholine (PC). Pi resonates in these spectra at 1 ppm. The phosphodiester resonances were identified as glycerophosphoethanolamine (GPE) and glycerophosphocholine (GPC) at 0.3 and −0.3 ppm, respectively. Most of the nucleotide triphosphates (NTPs) have been converted to Pi during the 1-min delay between killing the mice and placing the sample into liquid N_2.

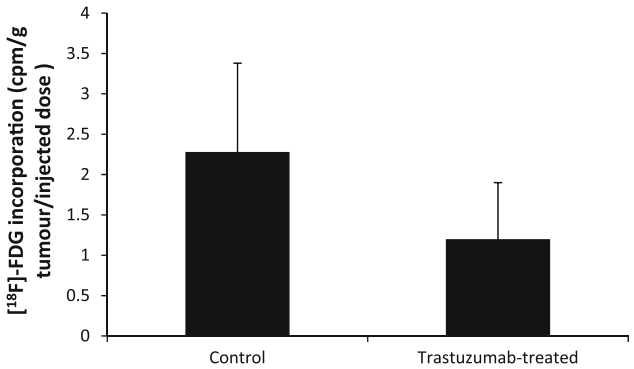

Fig. 2 [^{18}F]-FDG incorporation by MDA-MB-435 xenografts treated with trastuzumab for 15 days compared with xenografts grown in mice injected with PBS (control) (units: counts per minute (cpm) per gram tissue per MBq injected activity)

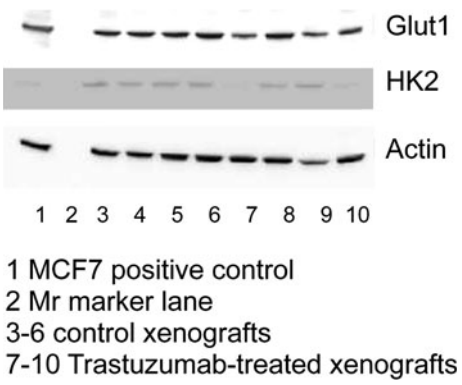

Fig. 3 Western blot showing lower expression of HK II and glut1 in trastuzumab-treated xenografts compared with non-treated xenografts

The mean (±SD) concentrations of ^{31}P-NMR-detectable metabolites in xenografts from the control ($n = 6$) and trastuzumab-treated mice ($n = 6$) are shown in Fig. 5. The concentrations of both PE ($t = 3.9$, $p < 0.005$) and PC ($t = 3.42$, $p < 0.01$) were significantly decreased in the tumours growing in mice treated with trastuzumab compared with tumours growing in PBS-treated control mice. The third (unidentified) peak in the PME region was also decreased, compared with controls, in the trastuzumab-treated group ($t = 2.32$, $p < 0.05$). The PME components are commonly quantified as a single peak in clinical studies. The PME resonances when summated were also significantly lower in concentration in tumours from the trastuzumab-treated group compared with the PBS-treated control mice.

The concentration of inorganic phosphorus + the high energy (HE) metabolites (peaks between −5 and −15 ppm) was not significantly different between the two groups ($t = 1.82$, ns), neither did the concentration of GPE ($t = 1.54$, ns) nor that of GPC ($t = 1.11$, ns) show any change with response.

To ensure that the decrease in concentration of the PMEs did not reflect a total fall in phosphorus signal in tumours from the trastuzumab-treated mice compared with the control group, their concentrations were expressed relative to total detectable phosphorus. When expressed relative to total phosphorus in each tumour, the mean (±SD) PE and PC content in tumours from the control tumours was 13.4 % (±1.3) and 15.04 % (±1.4) and from the trastuzumab-treated mice was 10.53 % (±1.7) ($t = 3.3$, $p < 0.01$) and 12.2 (±1.3) ($t = 3.7$, $p < 0.005$).

Discussion

The decision to treat breast cancer patients with trastuzumab is currently based on the HER2 status of their primary tumour which is determined using immunohistochemistry supplemented with fluorescent in situ hybridisation (FISH) for equivocal immunohistochemistry results [16]. There are a number of shortcomings associated with this approach, with respect to the technique utilised [17], the use of only primary tumour tissue [18, 19] and in some cancers the redundancy of HER2 in signal pathway activation [20]. Although FISH is commonly used to detect amplification of the HER2 gene, it will not identify the small percentage of breast tumours that do not exhibit gene amplification but overexpress HER2 receptor and could

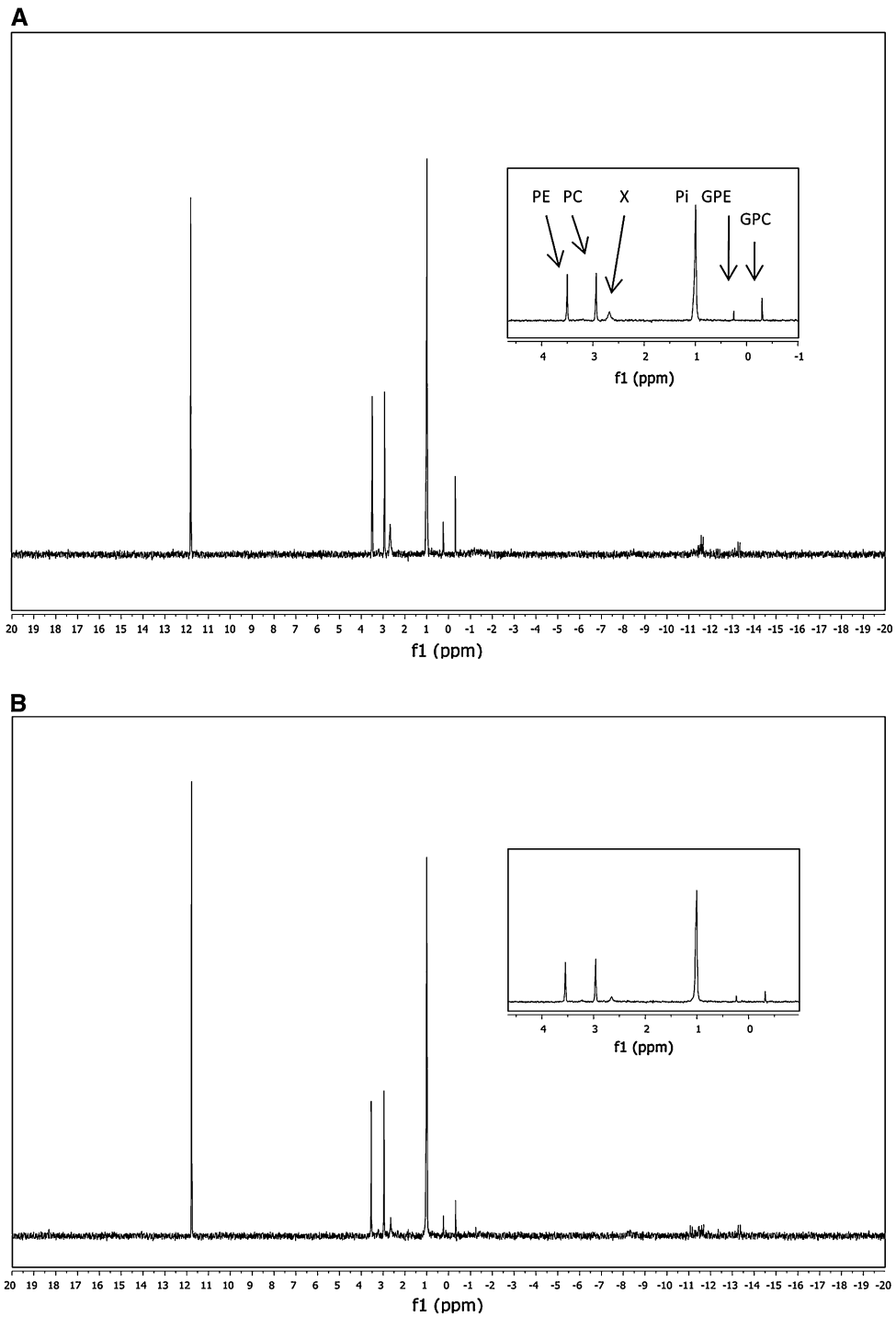

Fig. 4 **a** ^{31}P-NMR spectrum acquired from an aqueous extract of an MDA-MB-453 xenograft grown in mouse injected with PBS (control). **b** ^{31}P-NMR spectrum acquired from an aqueous extract of an MDA-MB-453 xenograft grown in a mouse treated for 15 days with trastuzumab

benefit from trastuzumab [17]. Several studies have shown that there is considerable discrepancy between the HER2 status of primary breast tumours and their secondary lesions so there is likely to be a subset of patients whose primary tumour is HER2 negative but axillary metastasis or recurrent/metastatic cancers [19] may respond to trastuzumab. However, in some tumours, the presence of HER2 may not indicate a therapy responsive tumour due to activating mutations in the Akt/PI3K pathway [20].

Both glucose [6] and phospholipid metabolism [21] can be influenced by the state of activation of the Akt pathway. In common with other tumour types, we demonstrated that the principal ^{31}P-NMR-detectable PMEs and PDEs in xenografts derived from MDA-MB-453 were the phospholipid metabolites PC and PE, and GPE and GPC, respectively [22]. The concentrations of both PC and PE were found to be significantly decreased in xenografts from the trastuzumab-treated mice compared with xenografts

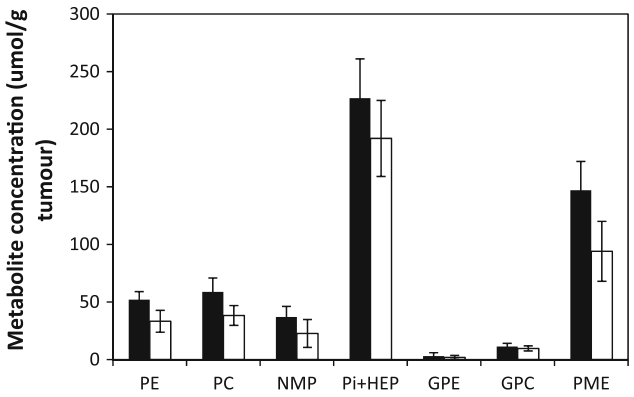

Fig. 5 Mean (error *bars* = standard deviation) content of ^{31}P-NMR spectroscopy-detectable metabolites in xenografts in PBS-injected mice (*black bars*) or trastuzumab-treated mice (*white bars*) (units: μmol/g tissue)

from vehicle (PBS)-treated mice. Tumours were excised and frozen by plunging into liquid nitrogen within 1 min of killing of each animal. During this time, most of the high energy phosphates, specifically the nucleoside phosphate, for example, ATP, will have been dephosphorylated hence the high levels of Pi in each tumour [23]. However, we have previously shown that PC, PE, GPC and GPE are stable in tumour tissue for up to 90 min after tumour excision [23].

Previous preclinical ^{31}P-NMR spectroscopy studies have also demonstrated that decreased levels of components of the PME region corresponds with response to both chemotherapy and anticancer agents targeting signalling pathways. Treatment of MCF-7 and MDA-MB-231 breast tumour xenografts with the antimicrotubule drug docetaxel resulted in significant decreases in tumour PC within 2–4 days post-treatment [24]. It has also been shown that treatment of breast tumour cells with the MAPK inhibitor U0126 [25] and treatment of human PC3 prostate and HCT116 colon carcinoma cells with the isoform-selective PI3K and mammalian target of rapamycin inhibitor PI-103 [21] was accompanied by decreased PC levels. The latter study demonstrated a concentration- and time-dependent decrease in PC and total choline (tCho) levels detected by ^{31}P- and ^{1}H-MRS [21], respectively. Decreased tumour content of tCho and in phospholipid metabolites including PC and PE have also been shown to correspond with response of HT-29 colorectal cells with the hypoxia-inducible transcription factor (HIF-1 alpha) inhibitor PX-478 [26].

A multi-institution ^{31}P-NMR spectroscopy study of non-Hodgkin's lymphoma (NHL) which carried out pre- and post-treatment ^{31}P-NMR scans reported that the phosphomonoesters (PME)/nucleotide triphosphates (NTP) ratio decreased significantly after treatment in complete ($p < 0.001$) and partial ($p < 0.05$) responders but not in non-responders ($p > 0.1$). In addition, the PME/NTP ratio in the pre-treatment spectra correlated with the subsequent outcome of treatment indicating that PME/NTP levels are significant predictors of long-term clinical response and time-to-treatment failure in NHL [27]. Despite these encouraging findings and the evidence from preclinical studies suggesting that ^{31}P-NMR spectroscopy is clinically useful, very few recent (in the past 10 years) studies have translated the technique to the clinic probably reflecting the low sensitivity of this technique. However, a recent study [28] has reported on the in vivo acquisition of ^{31}P-NMR spectra from glandular tissue of healthy volunteers and from patients with intraductal carcinomas using a 7-T whole body MR system and demonstrated that both PE and PC could be quantitated.

[^{18}F]FDG-PET is now well established as a tool for cancer management and is utilised in the diagnosis and staging of several cancer types and is also finding application in tumour response monitoring [29] where patients receive pre- and post-/during treatment scans. Patients responding to antiHER treatments including lapatinib [8], gefitinib [30] and erlotinib [31] exhibited decreased [^{18}F]FDG incorporation compared with pre-treatment. There are currently no clinical studies that have examined the effect of trastuzumab on [^{18}F]FDG incorporation.

The findings from preclinical studies are controversial and indicate that, whether or not response to trastuzumab is associated with changes in [^{18}F]FDG incorporation by HER-2 overexpressing tumour models is dependent on the tumour. Thus, our study using xenografts derived from MDA-MB-453 cells and a study [9] based on xenografts derived from MDA-MB-361 breast tumour cells have demonstrated that tumour [^{18}F]FDG incorporation decreases during response to this drug. However, treatment of xenografts derived from BT474 breast tumour cells and a transgenic murine cancer model with trastuzumab did not induce detectable changes in [^{18}F]FDG incorporation [10].

The rate limiting step for [^{18}F]FDG incorporation, which includes the rate of glucose transport and phosphorylation by hexokinase, differs between different tumours even of the same cancer type [32]. Thus, drug response will only induce changes in [^{18}F]FDG incorporation where the intervention modulates the activity of the rate limiting step. In MDA-MB-453 xenografts, we show that the protein expression of both HK II and glut1 are decreased in tumours responding to trastuzumab corresponding with decreased HK activity and glucose transport previously demonstrated in this cell line in vitro [33].

In addition to directly inhibiting intracellular signalling in HER2-overexpressing tumour cells, trastuzumab binding to HER-2 induces antibody-dependent cellular cytotoxicity (ADCC). SCID mice are deficient in both B and T lymphocytes but have macrophages and natural killer cells, so

they can still elicit the ADCC mechanism [34] although this effect can be higher in nude mice due to the presence of B cell response in nude mice compared with SCIDs [35]. Another aspect of species differences which may influence response to trastuzumab is its rate of clearance. In humans, the blood clearance of trastuzumab is about 19 days [36] and in mice has been shown to be about 10 days [37]. However, in the present study, mice were dosed every 2–3 days to maintain blood trastuzumab levels.

It has been shown that the biodistribution of [^{18}F]FDG is similar in animals injected i.p. and i.v. after 1 h [15]. We chose to administer the tracer i.p. as this is technically less challenging. However, this route would be inappropriate if the animals were undergoing a dynamic PET scan where tissue accumulation of [^{18}F]FDG is measured from the time of injection.

PET/MR hybrids capable of the simultaneous measurement of PET tracer distribution and MR imaging/spectroscopy have recently been developed [13]. These scanning devices would facilitate determination of [^{18}F]FDG incorporation and ^{31}P-NMR spectral acquisition in a single clinical session. Informing on both glucose utilisation and phospholipid metabolism compared with using only a single modality may provide a more accurate paradigm for the detection of response to trastuzumab.

In conclusion, we have shown that response of xenografts derived from MDA-MB-453 breast tumour cells to trastuzumab is accompanied by decreased ^{31}P-NMR-detectable PMEs and by decreased [^{18}F]FDG incorporation, the latter corresponding with decreased HK II and glut1 expression. As [^{18}F]FDG incorporation can be rate-limited by any of several factors, it is possible that changes in [^{18}F]FDG incorporation may not necessarily accompany response to biological agents such as trastuzumab so the co-employment of ^{31}P-NMR spectroscopy may provide a more accurate means of response assessment.

Acknowledgments This work was funded by the BBSRC and Breast Cancer research Campaign. NMR spectroscopy was carried out by Mr Russell Gray of the School of Natural Sciences and Computing at Aberdeen University.

Conflict of interest The authors declare they have no conflicts of interest.

References

1. Rousseau C, Devillers A, Sagan C, Ferrer L, Bridji B, Campion L et al (2006) Monitoring of early response to neoadjuvant chemotherapy in stage II and III breast cancer by [F-18]fluorodeoxyglucose positron emission tomography. J Clin Oncol 24:5366–5372
2. Berriolo-Riedinger A, Touzery C, Riedinger JM, Toubeau M, Coudert B, Arnould L et al (2007) [F-18]FDG-PET predicts complete pathological response of breast cancer to neoadjuvant chemotherapy. Eur J Nucl Med Mol Imag 34:1915–1924
3. Dunnwald LK, Gralow JR, Ellis GK, Livingston RB, Linden HM, Specht JM et al (2008) Tumor metabolism and blood flow changes by positron emission tomography: relation to survival in patients treated with neoadjuvant chemotherapy for locally advanced breast cancer. J Clin Oncol 26:4449–4457
4. Specht JM, Tam SL, Kurland BF, Gralow JR, Livingston RB, Linden HM et al (2007) Serial 2-[F-18] fluoro-2-deoxy-D-glucose positron emission tomography (FDG-PET) to monitor treatment of bone-dominant metastatic breast cancer predicts time to progression (TTP). Breast Cancer Res Treat 105:87–94
5. Jerome L, Alami N, Belanger S, Page V, Yu QN, Paterson J et al (2006) Recombinant human insulin-like growth factor binding protein 3 inhibits growth of human epidermal growth factor receptor-2-overexpressing breast tumors and potentiates Herceptin activity in vivo. Cancer Res 66:7245–7252
6. Paik JY, Ko BH, Jung KH, Lee KH (2009) Fibronectin Stimulates Endothelial Cell F-18-FDG Uptake Through Focal Adhesion Kinase-Mediated Phosphatidylinositol 3-Kinase/Akt Signaling. J Nucl Med 50:618–624
7. Kelly C, Smallbone K, Brady M (2008) Tumour glycolysis: the many faces of HIF. J Theoret Biol 254:508–513
8. Kawada K, Murakami K, Sato T, Kojima Y, Ebi H, Mukai H, Tahara M, Shimokata K, Minami H (2007) Prospective study of positron emission tomography for evaluation of the activity of lapatinib, a dual inhibitor of the ErbB1 and ErbB2 tyrosine kinases, in patients with advanced tumors. Jpn J Clin Oncol 37:44–48
9. McLarty K, Fasih A, Scollard DA, Done SJ, Vines DC, Green DE et al (2009) F-18-FDG small-animal PET/CT differentiates trastuzumab-responsive from unresponsive human breast cancer xenografts in athymic mice. J Nucl Med 50:1848–1856
10. Shah C, Miller TW, Wyatt SK, McKinley ET, Olivares MG, Sanchez V et al (2009) Imaging biomarkers predict response to Anti-HER2 (ErbB2) therapy in preclinical models of breast cancer. Clin Cancer Res 15:4712–4721
11. Griffiths JR, Tate AR, Howe FA, Stubbs M (2002) Magnetic resonance spectroscopy of cancer—practicalities of multi-centre trials and early results in non-Hodgkin's lymphoma. Eur J Cancer 38:2085–2093
12. Leach MO, Verrill M, Glaholm J, Smith TAD, Collins DJ, Payne GS, Sharp JC, Ronen SM, McCready VR, Powles TJ, Smith IE (1998) Measurements of human breast cancer using magnetic resonance spectroscopy: a review of clinical measurements and a report of localized P-31 measurements of response to treatment. NMR Biomed 11:314–340
13. Mansi L, Ciarmiello A, Cuccurullo V (2012) PET/MRI and the revolution of the third eye. Eur J Nucl Med Mol Imag 39:1519–1524
14. Plosker G, Keam S (2006) Trastuzumab: a review of its use in the management of HER2-positive metastatic and early-stage breast cancer. Drugs 66:449–475
15. Fueger BJ, Czernin J, Hildebrandt I, Tran C, Halpern BS, Stout D, Phelps ME, Weber WA (2006) Impact of animal handling on the results of 18F-FDG PET studies in mice. J Nucl Med 47:999–1006
16. Purdie CA, Jordan LB, McCullough JB, Edwards SL, Cunningham J, Walsh M et al (2010) HER2 assessment on core biopsy specimens using monoclonal antibody CB11 accurately determines HER2 status in breast carcinoma. Histopathology 56:702–707
17. Zhang D, Salto-Tellez M, Do E, Putti TC, Koay ESC (2003) Evaluation of HER-2/neu oncogene status in breast tumors on tissue microarrays. Hum Pathol 34:362–368
18. Aitken SJ, Thomas JS, Langdon SP, Harrison DJ, Faratian D (2010) Quantitative analysis of changes in ER, PR and HER2

expression in primary breast cancer and paired nodal metastases. Ann Oncol 21:1254–1261
19. Thompson AM, Jordan LB, Quinlan P, Skene A, Dewar JA, Purdie CA (2010). Prospective comparison of switches in biomarker status between primary and recurrent breast cancer: the Breast Recurrence In: Tissues Study (BRITS). Breast Cancer Res. 12 Article Number: R92
20. Faratian D, Goltsov A, Lebedeva G, Sorokin A, Moodie S, Mullen P et al (2009) Systems biology reveals new strategies for personalising cancer medicine and confirms the role of PTEN in resistance to trastuzumab. Cancer Res 69:6713–6720
21. Al-Saffar NMS, Jackson LE, Raynaud FI, Clarke PA, de Molina AR, Lacal JC et al (2010) The phosphoinositide 3-Kinase inhibitor PI-103 downregulates choline kinase a leading to phosphocholine and total choline decrease detected by magnetic resonance spectroscopy. Cancer Res 70:5507–5517
22. Leach MO (2006) Magnetic resonance spectroscopy (MRS) in the investigation of cancer at The Royal Marsden Hospital and The Institute of Cancer Research. Phys Med Biol 51:R61–R82
23. Smith TAD, Glaholm J, Leach MO, Machin L, McCready VR (1991) The effect of intra-tumor heterogeneity on the distribution of phosphorus-containing metabolites within human breast-tumors—an invitro study using p-31 nmr-spectroscopy. NMR Biomed 4:262–267
24. Morse DL, Raghunand N, Sadarangani P, Murthi S, Job C, Day S, Howison C, Gillies RJ (2007) Response of choline metabolites to docetaxel therapy is quantified in vivo by localized P-31 MRS of human breast cancer xenografts and in vitro by high-resolution P-31 NMR spectroscopy of cell extracts. Magn Reson Med 58:270–280
25. Beloueche-Babari M, Jackson LE, Al-Saffar NMS, Workman P, Leach MO, Ronen SM (2005) Magnetic resonance spectroscopy monitoring of mitogen-activated protein kinase signalling inhibition. Cancer Res 65:3356–3363
26. Jordan NF, Black K, Robey IF, Runquist M, Powis G, Gillies RJ (2005) Metabolite changes in HT-29 xenograft tumors following HIF-1 alpha inhibition with PX-478 as studied by MR spectroscopy in vivo and ex vivo. NMR Biomed 18:430–439
27. Griffiths JR, Tate AR, Howe FA, Stubbs M (2002) Magnetic resonance spectroscopy of cancer—practicalities of multi-centre trials and early results in non-Hodgkin's lymphoma. Eur J Cancer 38:2085–2093
28. Wijnen JP, van der Kemp WJM, Luttje MP, Korteweg MA, Luijten PR, Klomp DWJ (2012) Quantitative 31P magnetic resonance spectroscopy of the human breast at 7 T. Mag Resonan Med 68:339–348
29. Langer A (2010). A systematic review of PET and PET/CT in oncology: a way to personalize cancer treatment in a cost-effective manner? BMC Health Services Res. 10 Article Number: 283
30. Takahashi R, Hirata H, Tachibana I, Shimosegawa E, Inoue A, Nagatomo I, Takeda Y, Kida H, Goya S, Kijima T, Yoshida M, Kumagai T, Kumanogoh A, Okumura M, Hatazawa J, Kawase I (2012) Early [F-18]Fluorodeoxyglucose positron emission tomography at two days of gefitinib treatment predicts clinical outcome in patients with adenocarcinoma of the lung. Clin Cancer Res 18:220–228
31. Mileshkin L, Hicks RJ, Hughes BGM, Mitchell PLR, Charu V, Gitlitz BJ, Macfarlane D, Solomon B, Amler LC, Yu W, Pirzkall A, Fine BM (2011) Changes in F-18-Fluorodeoxyglucose and F-18-Fluorodeoxythymidine positron emission tomography imaging in patients with non-small cell lung cancer treated with erlotinib. Clin Cancer Res 17:3304–3315
32. Smith TAD (2001)The rate-limiting step for tumor [F-18]fluoro-2-deoxy-D-glucose (FDG) incorporation. Nucl Med Biol 28:1–4
33. Cheyne RW, Trembleau L, McLaughlin AC, Smith TAD (2011) Changes in 2-Fluoro-2-deoxy-D-glucose incorporation, hexokinase activity and lactate production by breast cancer cells responding to treatment with the anti-HER-2 antibody trastuzumab. Nucl Med Biol 38:339–346
34. Hasui M, Saikawa Y, Miura M et al (1989) Effector and precursor phenotypes of lymphokine-activated killer cells in mice with severe combined immunodeficiency (SCID) and athymic (nude) mice. Cell Immunol 120:230–239
35. Barok M, Isola J, Palyi-Krekk Z, Nagy P, Juhasz I, Vereb G et al (2007) Trastuzumab causes antibody-dependent cellular cytotoxicity-mediated growth inhibition of sub macroscopic JIMT-1 breast cancer xenografts despite intrinsic drug resistance. Mol Cancer Therapeut 6:2065–2072
36. Leyland-Jones B, Gelmon K, Ayoub JP, Arnold A, Verma S, Dias R, Ghahramani P (2003) Pharmacokinetics, safety, and efficacy of trastuzumab administered every three weeks in combination with paclitaxel. J Clin Oncol 21:3965–3971
37. Zhang NY, Liu LM, Dumitru DT et al (2011) Glycoengineered Pichia produced anti-HER2 is comparable to trastuzumab in preclinical study. MABS 3:289–298